

Mechanics unlocks the morphogenetic puzzle of interlocking bivalved shells

Derek E. Moulton^{a,2}, Alain Goriely^a, and Régis Chirat^b

^aMathematical Institute, University of Oxford, Oxford, UK; ^bCNRS 5276, Université Lyon 1, 69622 Villeurbanne Cedex, France

This manuscript was compiled on November 27, 2019

1 Brachiopods and mollusks are two shell-bearing phyla that diverged
2 from a common shell-less ancestor more than 540 million years ago.
3 Brachiopods and bivalve mollusks have also convergently evolved a
4 bivalved shell that display an apparently mundane, yet striking fea-
5 ture from a developmental point of view: when the shell is closed,
6 the two valve edges meet each other in a commissure that forms a
7 continuum with no gaps or overlaps despite the fact that each valve,
8 secreted by two mantle lobes, may present antisymmetric ornamen-
9 tal patterns of varying regularity and size. Interlocking is maintained
10 throughout the entirety of development, even when the shell edge
11 exhibits significant irregularity due to injury or other environmental
12 influences, which suggests a dynamic physical process of pattern
13 formation that cannot be genetically specified. Here, we derive a
14 mathematical framework, based on the physics of shell growth, to
15 explain how this interlocking pattern is created and regulated by me-
16 chanical instabilities. By close consideration of the geometry and
17 mechanics of two lobes of the mantle, constrained both by the rigid
18 shell that they secrete and by each other, we uncover the mecha-
19 nistic basis for the interlocking pattern. Our modeling framework
20 recovers and explains a large diversity of shell forms and highlights
21 how parametric variations in the growth process result in morpho-
22 logical variation. Beyond the basic interlocking mechanism, we also
23 consider the intricate and striking multiscale patterned edge in cer-
24 tain brachiopods. We show that this pattern can be explained as a
25 secondary instability that matches morphological trends and data.

morphogenesis | growth | mathematical model | mollusk

1 **B**rachiopods and mollusks are two invertebrate phyla that
2 possess calcified shells. Evidence derived from molecular
3 clocks, molecular phylogeny, shell biochemistry and from the
4 fossil record (? ? ? ? ?) suggest however that they
5 have diverged from a shell-less common ancestor (Fig. 1).
6 The bivalved condition of the shell in both brachiopods and
7 bivalve mollusks is an evolutionary convergence that led several
8 authors to mistakenly assign brachiopods to mollusks in the
9 early 19th century (?). One of the most remarkable features
10 of the shells of brachiopods and bivalves, readily observed
11 but rarely fully appreciated, is the simple fact that the two
12 valves of the shell fit together perfectly when the shell is
13 closed, i.e. throughout the development of the shell the edge
14 of two valves meet each other in a commissure that forms a
15 continuous curve with no gaps. At first glance this may not
16 appear as a surprise, as the two valves comprise two halves
17 of the same organism. Moreover, it is a trait that brings an
18 easily understood functional advantage, providing a protective
19 role against predators and environmental events, and it could
20 be tempting to conclude that this function alone explains why
21 both valves closely interlock. However, the function of a trait
22 does not explain how it is formed during development, which
23 is the goal of the present work.

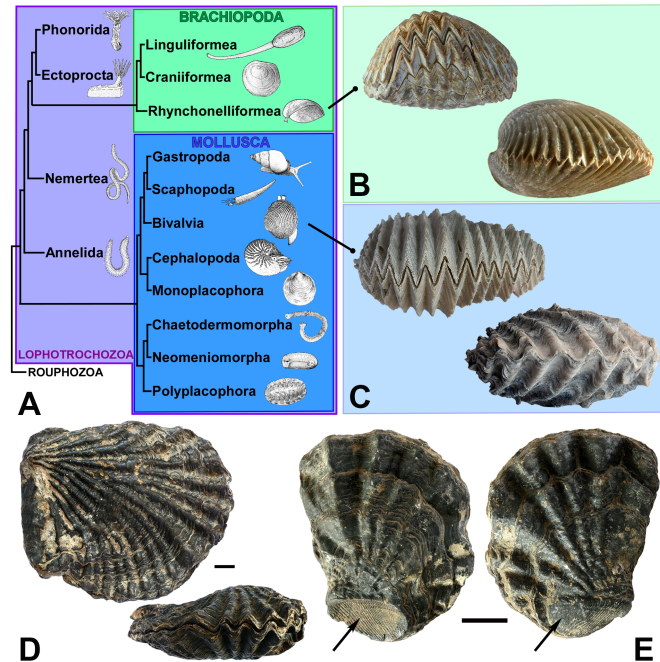


Fig. 1. A. Phylogenetic relationships among brachiopods and mollusks (modified after (? ? ?)). B-C Convergently evolved shell commissures in fossil brachiopods (*Septaliphoria orbignyana*; *Kutchirhynchia obsoleta*) and bivalve mollusks (*Rastellum sp.*; *Ctenostreon rugosum*). D. An oyster with irregular interlocking pattern, *Lopha sp.* (Senonian, Algeria). E. Xenomorphic oyster, *Lopha sp.* (Upper Cretaceous, Algeria); the attached valve carries the negative impression of another shell, while the free valve replicates its positive form (as indicated by the arrows).

The two valves of the shell are secreted separately by two lobes of a thin elastic organ, the mantle. Also, the two valves may grow at different rates, have different shapes, and the pattern of shell edge does not exhibit perfect regularity: it may be more or less perturbed, for instance by external factors such as a patterned substrate on which some species live attached, or by environmental events causing shell injuries. Yet, in all cases the interlocking of the two shell edges is tightly maintained. These observations imply that the interlocking pattern emerges as the result of epigenetic interactions modulating the behavior of the secreting mantle during shell development.

Here, we provide a geometric and mechanical explanation for this morphological trait based on a detailed analysis of the shell geometry during growth and the physical interaction of the shell-secreting soft mantle with both the rigid shell edge and the opposing mantle lobe. We demonstrate how an interlocking patterned shell edge emerges naturally as the continuation of a biaxially constrained mechanical instability. We demonstrate how significant morphological variation emerges via parametric variation, and also demonstrate how

44 a secondary instability accounts for the striking multi-scaled
45 oscillatory patterns found on certain brachiopods.

46 1. Background

47 Despite some differences in mode of secretions and anatomy
48 between bivalves and brachiopods, the shells of both groups
49 are incrementally secreted at the margin by a thin membra-
50 nous elastic organ called the mantle, that secretes first the
51 periostracum, a thin soft organic layer that serves as a matrix
52 for the deposition of the calcium carbonate of the shell (?
53 ?). The form of the calcified shell may thus be viewed as
54 a spatiotemporal record of the form taken by the mantle at
55 the shell margin during development. Though recent studies
56 have begun to investigate cellular differential growth patterns
57 underlying left-right asymmetries in gastropods (?) or to
58 identify genetic and molecular bases of shell biomineralization
59 in both mollusks and brachiopods (? ?), the morphogenetic
60 processes underlying the diversity of shell shapes in both
61 groups remains poorly known. Theoretical models invoking
62 either reaction-diffusion chemical systems (?) or nervous
63 activity in the mantle epithelial cells (?), though success-
64 ful in capturing the emergence of pigmentation patterns, do
65 not explain the emergence of three-dimensional forms. A
66 common default assumption in developmental biology is that
67 molecular patterning precedes and triggers three-dimensional
68 morphogenetic processes. While this assumption might partly
69 motivate recent studies of genetic and molecular mechanisms
70 involved in shell development, only two-dimensional pigmenta-
71 tion patterns (that are molecular in nature) have been shown
72 to map precisely with gene expression patterns (?). Marginal
73 shell growth in bivalves and brachiopods takes place when the
74 valves are open, both mantle lobes being retracted away from
75 the margin of each valve when the shell is tightly closed. In
76 the case of patterned interlocking commissures, it is difficult
77 to conceive of genetic and molecular processes of morpho-
78 genetic regulation that would specify that when the margin
79 of a mantle lobe secretes a patterned edge on one valve, the
80 same complex processes must regulate the morphogenesis of
81 the other mantle lobe to generate a perfectly antisymmetric

edge on the other valve, both patterned edges closely inter-
locking when the mantle is retracted and the shell is closed.
In other words, supposing that molecular patterning triggers
three-dimensional morphogenetic processes raises the question
of the nature of the coordinating signal between both mantle
lobes and how it could be transmitted. Formulated in that
way, the development of closely interlocking edges, and the
repeated emergence of similar complex commissures during
the evolution of two different phyla, are puzzling problems.

A partial answer to this puzzle comes from oysters that
live attached to a substratum. In these oysters, the surface
of the attached valve carries the negative impression of the
morphology of the substratum, while the free valve replicates
in positive the form of the substratum, a phenomenon known
as xenomorphism (i.e. 'having a foreign form') (Fig.1E). No
matter the irregular form of the substratum on which the
oyster is attached (a stone, another shell, an artificial sub-
strate), the edge of the free valve closely fits with the edge of
the attached valve. As the oyster grows bigger, the mantle
margin of the attached valve starts to turn away from the
substratum, and no longer grows attached. At this stage, the
shell attains what is called its idiomorphic form (i.e. 'having
its own form') (?) and in some species, a zigzag-shaped
commissure is generated at this stage. Our interpretation
is that the xenomorphic and idiomorphic parts do not differ
fundamentally from the point of view of the growth processes.
In the xenomorphic part, the form taken by the mantle margin
secreting the attached valve is mechanically imposed by the
form of the substratum, and this form is itself mechanically
imposed to the mantle lobe secreting the free valve when both
mantle lobes are at least temporarily in close contact while
secreting the slightly opened shell. Once the shell no longer
grows attached to the substratum, the mechanical influence
of the substratum is removed and there is only a reciprocal
mechanical influence between both lobes. This reciprocal me-
chanical influence seems to be a general characteristic of the
growth of brachiopods and bivalves. For example, in the case
of traumatic individuals, the non-traumatic valve adapts its
form and interlocks with the traumatic valve, no matter the

Significance Statement

A striking feature in bivalved seashells is that the two valves fit together perfectly when closed. This trait has evolved in two phyla from a common shell-less ancestor and has been described for hundreds of years. While its functional advantage is clear, there is no understanding on how this feature is generated. A mathematical model of the shell growth process explains how geometry and mechanics conspire to generate an interlocking pattern. This model provides a physical explanation for a prominent example of convergent evolution. By showing how variations in the mechanism create a wide variety of morphological trends the model provides insight into how biophysical processes, probably modulated by genetic factors, are manifest across scales to produce a predictable pattern.

DEM and RC conceived the study. DEM and AG devised the mathematical model. Computations were performed by DEM. Shells were obtained and photographed by RC. DEM collected data on shell asymmetry. All authors contributed to the writing of the paper.

We have no conflict of interest.

²To whom correspondence should be addressed. E-mail: moulton@maths.ox.ac.uk

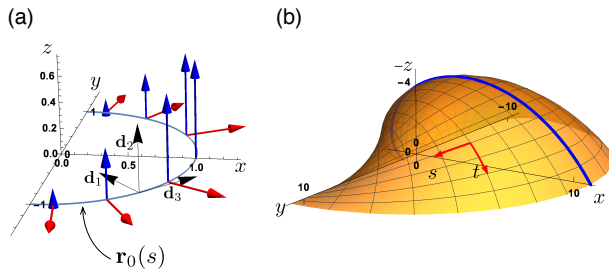


Fig. 2. (a) The base geometry for bivalved shells is constructed via a locally defined growth velocity field defined on a base curve $\mathbf{r}_0(s)$ equipped with orthonormal basis $\{\mathbf{d}_1, \mathbf{d}_2, \mathbf{d}_3\}$. The growth consists of dilation (red arrows) and a coiling velocity in the binormal (\mathbf{d}_2) direction with linear gradient (blue arrows) and hinge along the y -axis. (b) The resulting surface for one valve of the bivalve shell, with the s and t directions highlighted as well as the longitudinal midline (the curve $s = 0$), which forms a logarithmic spiral.

binormal growth velocity component $q_2 = bx_0(s)$; i.e. shell 163
 coiling requires a linear growth gradient along an axis (taken 164
 without loss of generality to be the initial x -axis). Bivalves 165
 also require a hinge; in this formulation the hinge is the y -axis, 166
 where $x_0 = 0$ and thus $q_2 = 0$; see Fig. 2 and further geometric 167
 details in Supplementary Information (SI) Appendix Section 1. 168
 The benefit of this approach is that the base shape of the 169
 shell emerges through a single geometric growth parameter, 170
 the coiling rate b that can be related to a self-similar process 171
 of secretion of shell material and growth of the mantle. We do 172
 not assume a symmetry between the two valves, i.e. the coiling 173
 rates for the two halves may be different as seen in brachiopods 174
 (see Section 3C). Nevertheless, due to fixed dilation ($c = 1$ for 175
 both valves), if both halves have the same initial curve then 176
 the two valves (of the smooth shell) will always meet perfectly 177
 in the x - y plane when the base shell is closed. 178

B. Mechanical basis of ornamentation. In bivalves and bra- 179
 chiopods, three-dimensional ornamentations typically consist 180
 of an oscillation pattern of the shell edge that is termed *anti-* 181
marginal ornamentation. The basic premise for our investi- 182
 gation is that while the developmental processes underlying 183
 the variations of base geometry of the shell remain largely 184
 unknown, ornamentations emerge as the result of mechanical 185
 deformations of the secreting mantle margin (?). If the 186
 mantle grows at the same rate as the shell edge that it is 187
 itself secreting, both mantle and shell are in perfect synchrony 188
 and the shell will remain smooth. However, if the mantle 189
 margin grows faster, it has an excess of length with respect 190
 to the shell edge. This leads to a compressive stress that 191
 can induce buckling of the mantle, and the buckled pattern 192
 will subsequently be calcified in the next secretion of shell 193
 edge. If an excess of length is sustained through development, 194
 the deformation pattern will evolve and be amplified. In this 195
 way, ornamentation patterns are spatiotemporal records of 196
 these continued deformation patterns. This basic mechanism 197
 underlies the formation of ornamentation in shells and can be 198
 elegantly modeled by treating the mantle edge as a growing 199
 elastic beam (the mantle) attached to an evolving foundation 200
 (the rigid shell edge). Within this framework, one can explain 201
 how basic changes in shell geometry, growth, and mechanical 202
 properties produce a diverse morphology of ornamentation pat- 203
 terns (? ? ? ?). Here, we use the same modeling framework 204
 adapted to the growth constraints in bivalved shells. 205

C. Ornamentation orientation. In our model the shell is ob- 206
 tained as the superposition of the morphological pattern of 207
 the buckled mantle on the smooth geometric surface generated 208
 via the growth velocity field. Antimarginal ornamentation is 209
 generally understood as a morphological pattern in the plane 210
 orthogonal to the shell margin, i.e. in the plane which has 211
 normal vector pointing tangent to the direction of shell growth 212
 (the plane with normal vector $\dot{\mathbf{r}}$ in the geometric description 213
 outlined above). However, close inspection of bivalved seashells 214
 shows that ornamentations typically do not form in the or- 215
 thogonal plane and a natural problem is to determine the 216
 orientation of the ornamentation plane. Fig. 3(a) illustrates 217
 an oscillation pattern in the antimarginal plane as well the 218
 same pattern in a rotated plane. 219

The solution to this problem is the first key component 220
 that produces interlocking. The length of shell in the growth 221
 direction (i.e. arclength in the t -direction for fixed material 222

121 abnormal form of the shell edge.

122 Xenomorphic-idiomorphic transition in oysters and trauma
 123 mirroring in both bivalves and brachiopods suggest the fol-
 124 lowing hypothesis: *interlocking commissures are created by a*
 125 *combination of the mechanical constraints acting on each lobe*
 126 *and the mechanical influence of the two lobes on each other.*
 127 In this paper, we develop a theoretical model of shell morpho-
 128 genesis that confirms this hypothesis and extract universal
 129 morphogenetic rules. We show that the mechanical constraint
 130 acting on each lobe during growth imposes the geometric ori-
 131 entation of the morphological pattern while the reciprocal
 132 interaction between lobes enforces the antisymmetry of this
 133 pattern. Both principles are needed for perfect closure and
 134 are universal characteristics of the growth of brachiopods and
 135 bivalves.

136 2. Mathematical model

137 **A. Base Geometry.** We first describe the general framework
 138 for the growth of bivalved shells by using the localised growth
 139 kinematics description of (? ?). The shell is modeled as
 140 a surface $\mathbf{r} = \mathbf{r}(s, t) \in \mathbb{R}^3$, where s is a material parameter
 141 describing location along the shell edge, and t is a growth “time”
 142 parameter which need not correspond to actual time but which
 143 increases through development. The shell is constructed by
 144 defining an initial curve $\mathbf{r}(s, 0) = (x_0(s), y_0(s), 0)$ (where s is
 145 the arclength) and a growth velocity field $\mathbf{q}(s, t)$ representing
 146 the rate of shell secretion such that $\dot{\mathbf{r}} = \mathbf{q}$, (overdot represents
 147 time derivative). In the case of bivalved shells, the field \mathbf{q}
 148 requires only two components: a dilation rate, denoted c ,
 149 which describes the rate of expansion of the aperture, and a
 150 coiling rate, denoted b , which is equivalent to the gradient
 151 in growth in the binormal direction and dictates how tightly
 152 coiled the shell is (see Fig 2). However, since we are only
 153 interested in the shape we can set the dilation rate to $c = 1$
 154 without loss of generality, as it is only the ratio of dilation
 155 to expansion that is relevant in the shell form.

156 The key to this description is to express the velocity field in
 157 a local orthonormal basis $\{\mathbf{d}_1, \mathbf{d}_2, \mathbf{d}_3\}$ attached to each point
 158 of the shell edge. Here, we choose \mathbf{d}_3 to be tangent to the shell
 159 edge, i.e. $\mathbf{r}'(s, t) = \lambda(t)\mathbf{d}_3$, where prime denotes derivative
 160 with s and λ is a scale parameter characterizing the degree
 161 of total dilation from the base curve. Defining \mathbf{d}_2 to align
 162 with the binormal direction, coiling is generated through a

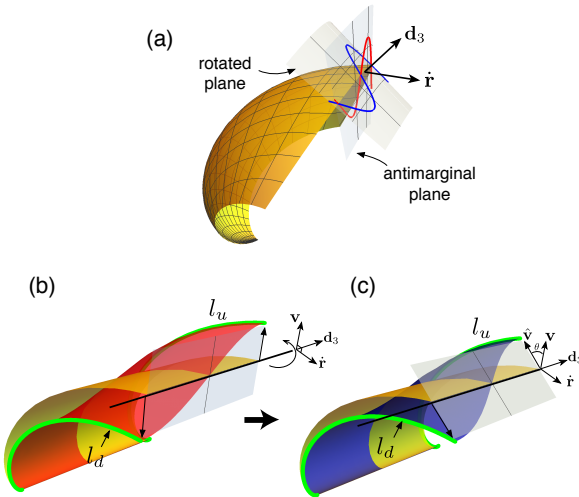


Fig. 3. (a) The difference between pattern imposed in the antimarginal plane, with normal vector \hat{r} , and a rotation of this plane about the \mathbf{d}_3 direction. In (b), an oscillatory pattern in the antimarginal plane creates an unbalanced strain in the generative zone, as the arclength at the valleys is less than at the peaks. In the schematic, the green curve l_d has shorter length l_u . This strain creates locally a moment around the \mathbf{d}_3 axis. (c) This moment is balanced by rotating the plane of ornamentation until the arclengths are made equal and the strain balanced.

point s) is determined by the rate of secretion. For neighboring material points the rate of secretion and thus arclength in the smooth shell are nearly identical. Once the mantle (and thus the shell edge) deforms, these arclengths may differ, depending on the plane in which the deformed pattern appears, and this will produce a moment of force about the shell edge (the \mathbf{d}_3 direction) that serves to rotate the plane. The idea is illustrated in Fig. 3(b)-(c). Fig. 3(b) shows a portion of a base shell (yellow), and the same shell with a half-mode oscillation pattern imposed on top (red), with the pattern appearing in the antimarginal plane.* Once the mantle deforms, however, the arclengths are no longer equal: the arclength at the point which has deformed “up” is longer than the arclength at the point which has deformed “down”, i.e. $l_u > l_d$ as pictured. This difference creates a differential strain in the generative zone, the deformable region that connects the mantle to the already calcified portion of the shell, which induces a moment of force acting on the mantle that rotates the plane of ornamentation. In Fig. 3(c), the same mode of deformation is shown in a rotated plane where the arclength at the “up” and “down” points are equal, $l_u = l_d$, so that the differential strain and thus the moment vanishes.

The precise degree of rotation that balances the strain depends on the stage of development, the material point along the shell edge, and the growth parameters for the base shell. In particular it is worth noting that the steeper the angle of commissure, which occurs with increased coiling rate b , the more rotation is needed. This is intuitive, if one considers that for a perfectly flat shell there is a perfect symmetry between “up” and “down” deformations, and thus no rotation is needed. Mathematically, points on the upper and lower side

*Locally, a small section of shell can be approximated as a cylinder with logarithmic spiral shape and with equal arclength at neighboring points prior to mantle deformation, hence for visual simplicity here we plot portions of the shells as being cylindrical.

of the pattern are located at $\mathbf{r}_{\text{up,down}} = \mathbf{r} \pm \epsilon \lambda \hat{\mathbf{v}}$ where ϵ is the amplitude of deflection of the mantle, the factor λ accounts for the scaling of the buckling pattern’s amplitude, and $\hat{\mathbf{v}}$ is a unit vector to be determined that describes the orientation of the pattern such that the ornamentation appears in the \mathbf{d}_3 - $\hat{\mathbf{v}}$ plane (details in SI Appendix Section 2). Then the balance of moment can be written as a geometric condition

$$\hat{\mathbf{r}} \cdot (\lambda \hat{\mathbf{v}} + \lambda \hat{\mathbf{v}}) = 0. \quad [1]$$

This is a nonlinear differential equation satisfied by the rotation angle, which will depend on both the material point s and the development time t .

D. Rule 1: Coplanarity of ornamentation planes. For perfect interlocking to occur, the pattern on each individual valve must locally occur in the same plane when the valve is closed. We state this as the first rule of interlocking: *the ornamentation planes of the two opposing valves must be aligned at all points when the valves are closed.* This geometric rule is illustrated in Fig. 4, in which we superimpose a sinusoidal ornamentation on a bivalve. In Fig. 4(a) the ornamentation is truly antimarginal, i.e. there is no rotation of the plane of ornamentation. In this case, even though the pattern on the two valves was chosen to coincide, i.e. the sinusoidal curves are in phase, significant gaps and overlaps appear so that the valves do not interlock. Fig. 4(b) shows the same shell, but with a rotation of the plane of ornamentation. Here, a perfect interlocking is attained. Intuitively, the reason that the two valves can interlock is that the rotation imposed by generative zone strain causes both patterns to develop *in the same plane.*

The argument and calculation in Section C provides a geometric condition for the local orientation of the plane of each valve, though it is to be noted that this condition does not take into account the presence of the other valve. However,

286 when both valves are rotated to meet in the x - y plane, Rule 1
 287 is satisfied. Indeed, the plane of ornamentation for the shell in
 288 Fig. 4(b) was computed according to the calculation described
 289 above. In fact we find that this is a generic feature: for a
 290 bivalved shell growing according to the rules outlined above,
 291 and with plane of ornamentation defined by the balance of
 292 moments Eq. (1), the planes of ornamentation of each valve
 293 almost perfectly coincide at all points along the shell edge and
 294 at all times throughout development (see Section 2 of SM).

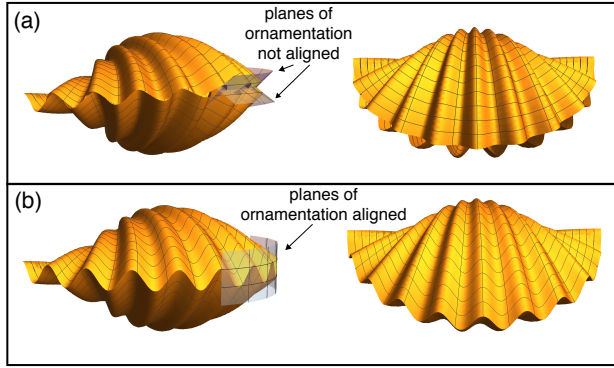


Fig. 4. The first rule of interlocking: At the shell level rotating the ornamentation plane is important for interlocking. A non-rotated plane of ornamentation (a) leads to a misalignment of the ornamentation patterns and thus gaps and overlaps appear when the two valves are closed. With rotation (b), opposing planes agree and a perfect interlocking is attained.

E. Rule 2: In-phase synchrony of ornamentation pattern.

295 While the coplanarity of ornamentation planes ensures that
 296 the two ornamentation patterns will appear in the same plane,
 297 it does not in itself guarantee that the two valves will interlock.
 298 For this to occur, we also require Rule 2 of interlocking: *the*
 299 *ornamentation patterns must coincide in phase*. We now show
 300 that this synchrony is born out of the mechanical interaction
 301 of the two opposing mantle lobes.

302 Following (? ?), we treat each mantle edge as a morpho-
 303 elastic rod (? ?) attached elastically via the generative zone to a
 304 foundation, the rigid calcified shell (see details in SI Appendix
 305 Section 3). The two mantle edges interact with each other
 306 when in contact through a repulsive interaction force ensuring
 307 that the two mantles cannot interpenetrate.

308 Since the two valves are meeting at a common plane with
 309 equivalent length of shell edge, and assuming that the mantle
 310 tissue of each valve has the same mechanical properties, given
 311 an excess of length that induces a mechanical pattern, the
 312 preferred buckling mode for each respective valve will be the
 313 same, if considered in isolation. The question then is what
 314 form the buckled pattern will take when the two mantle edges
 315 are not in isolation, but interacting with each other. The
 316 problem is greatly simplified by the first rule: since the two
 317 planes of ornamentation are locally aligned, we can consider
 318 the buckling problem in a single surface. Further assuming
 319 that the curvature of the mantle along the edge is small, we
 320 ‘unwrap’ the common ornamentation surface and consider a
 321 planar problem. For a given excess of length due to mantle
 322 growth, we compute the possible modes of deformation for the
 323 two mantles parametrically given by $(x_i(s), y_i(s))$, $i = 1, 2$,
 324 in the x - y ornamentation plane (SI Appendix Section 3). Once
 325 these are found, we consider the total mechanical energy of the
 326

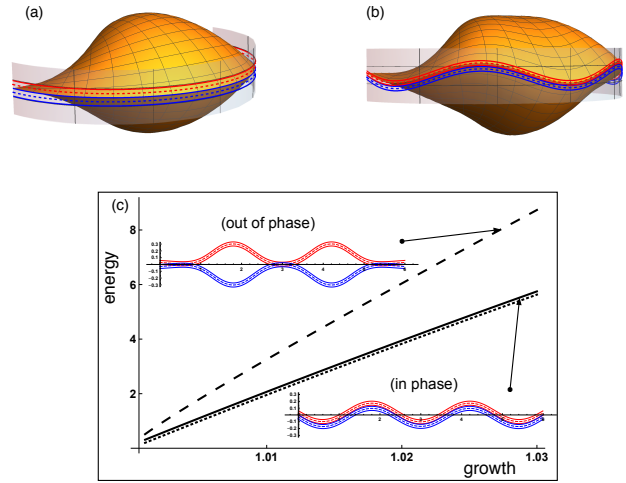


Fig. 5. The ornamentation pattern emerges as a mechanical instability due to excess growth of the shell secreting mantle and periostracum. In the model, the mantle edge (a) is “unwrapped” to compute the 2D pattern which is then imposed back on the shell in the plane of ornamentation (b). In (c), an energy comparison demonstrates that the “in phase” pattern with interlocking edges is energetically favorable and nearly identical to the energy without interaction between the mantles (dotted curve in (c)).

system, given by the sum of bending and foundation energies
 on each side and the interaction energy between the two:

$$\mathcal{E} = \mathcal{E}_{\text{bend}}^{(1)} + \mathcal{E}_{\text{bend}}^{(2)} + \mathcal{E}_{\text{found}}^{(1)} + \mathcal{E}_{\text{found}}^{(2)} + \mathcal{E}_{\text{interaction}} \quad [2]$$

where

$$\mathcal{E}_{\text{bend}}^{(i)} = \frac{1}{2} m_i(s)^2, \quad \mathcal{E}_{\text{found}}^{(i)} = \frac{k}{2} (y_i(s) - (-1)^i \delta)^2. \quad [3]$$

Here δ denotes the half-width of each mantle, m_i is the resultant moment acting on the growing mantle, and k describes the strength of the foundation. The interaction between both mantles is

$$\mathcal{E}_{\text{interaction}} = f((y_1 - y_2) - 2\delta)^{-2}, \quad [4]$$

where f is a constant that characterises the strength of the repulsive interaction. We compare the energy in two distinct configurations: one in which the opposing mantle edges are “in phase”, and one in which they are “out of phase”. These configurations are obtained by first computing the preferred buckling shape of a mantle in isolation. The buckling forms a bifurcation from the trivial straight solution with two solution branches of equal energy that are mirror images of each other. Taking both mantles from the same branch forms the “in-phase” solution while taking them from opposing branches forms the “out-of-phase” solution. We then compute the energy in the system as a function of mantle growth. The energies are plotted in Fig. 5(c), which shows that the energy in the “out of phase” pattern is significantly higher than the “in phase” energy. For comparison, we compute the energy of the two mantles in the absence of interaction (dashed line), which forms a lower bound on the total energy.

The complete shell with the energy minimising buckling pattern imposed is plotted in Fig. 5(b). Physically, the “in phase” pattern has lower energy because a large deformation is needed to maintain geometric compatibility in the “out of phase” case, and the contact energy is also much higher. The significant difference in energy between “in phase” and “out of

360 phase” deformation modes (almost double at the point of only
 361 3% growth extension) and the close proximity of “in-phase”
 362 energy with the lower bound “no interaction” energy, suggests
 363 that the “in phase” solution is a global minimizer and the
 364 preferred configuration. We conclude that the mechanical
 365 interaction of the mantles provides the mechanism for Rule 2.

366 3. Morphological trends

367 **A. Growth, accretion, and secretion.** The formation of a shell
 368 involves three distinct but closely related activities: growth
 369 of the mantle, secretion of new shell material by the mantle,
 370 and accretion of the shell. The distinction between secretion
 371 and accretion is subtle, but if we define accretion as increase
 372 of shell length in the growth direction, then it becomes clear
 373 that it is possible for shell material to be secreted without
 374 actually contributing to accretion, e.g. by thickening the shell
 375 as empirical evidence shows in many seashells. To explain the
 376 distinction between observed morphologies requires considering
 377 the interplay between these activities.

378 We first consider the link between mantle growth and se-
 379 cretion rate. By mantle growth we refer specifically to lon-
 380 gitudinal growth along the mantle edge – the growth that
 381 produces the excess of length that drives mantle buckling and
 382 thus generates the patterned shell edge. The rate of ampli-
 383 fication of the buckling pattern is governed by the rate of
 384 mantle growth. Here we make the simple assumption that
 385 the mantle growth rate is proportional to the secretion rate b . In
 386 this way, a shell with higher coiling rate (larger b) will have
 387 a higher ornamentation amplitude compared to a shell with
 388 lower coiling rate. In particular, the linking of growth with
 389 secretion provides a simple mechanism for zigzag commissures
 390 (see Fig. 1C), which tend to appear in shells with very steep
 391 angle of commissure (high coiling rate): these may be seen as
 392 an extreme form of a (smooth) buckling pattern but with a
 393 very small wavelength combined with a high amplitude, the
 394 latter arising due to high secretion rate.

395 **B. A 2D morphospace.** In this construction, there are only two
 396 main parameters governing the shell morphology: the coiling
 397 rate b , and a single mechanical parameter k (see SI Appendix
 398 Section 3), which governs the mode of buckling and hence the
 399 wavelength of the interlocking ornamentation pattern[†].

400 In Fig. 6 we illustrate the range of shell morphologies as a 2D
 401 morphospace formed by the parameters k and b . A low value
 402 of k results in a long wavelength pattern, and vice versa, while
 403 a low coiling rate produces a shallow shell, with high coiling
 404 rate producing a steeper shell and more amplified pattern. For
 405 comparison, we include four representative shells matching the
 406 basic characteristics of each corner of the morphospace. Since
 407 by construction these shells satisfy both rules of interlocking,
 408 the interlocking pattern is perfectly formed.

409 **C. Asymmetry and secondary ornamentation.** An intriguing
 410 feature of our findings is that interlocking does not require
 411 symmetry between the two valves (consider: your two hands
 412 clasp together very nicely, but they also grow as almost perfect
 413 mirror images). Indeed, in many shells, notably in brachiopods,
 414 the two valves have markedly different coiling rates. In our

[†]The cross-sectional shape is another degree of freedom, and indeed our approach may be applied to any cross-sectional shape, but we have restricted to a semi-circle here, as this provides the simplest form and is a good model for most bivalved shells.

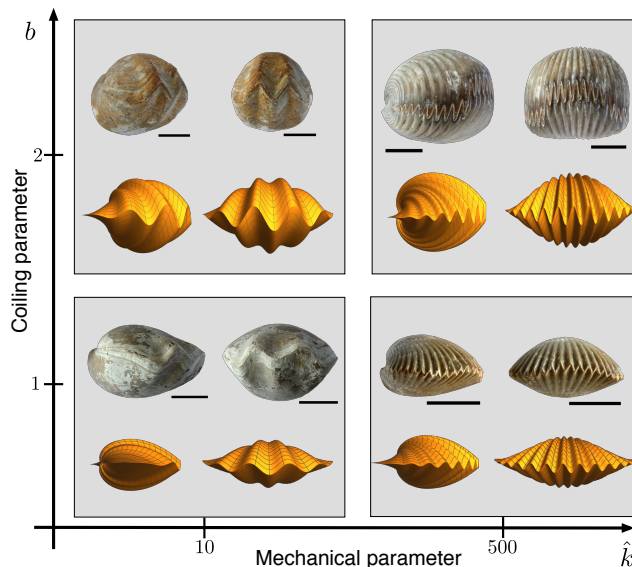


Fig. 6. Morphology variety for (symmetric) interlocking bivalved shells and sample shells illustrating the diversity of form. The simulated shells correspond to the 4 different combinations of a low ($b = 1$) and high ($b = 2$) coiling rate and small ($k = 10$) and large ($k = 500$) mechanical stiffness. The computational procedure is outlined in SI Appendix Section 4.

model, Rule 1 is accomplished by a rotation of the generative zone that does not rely on the physical interaction of the opposing valve, thus the two base valves need not be mirror images of each other for the planes of ornamentation to align. And once the planes align, Rule 2 for antisymmetry of the pattern is accomplished by the mechanical interaction of the two mantles.

However, by linking mantle growth to secretion rate, an asymmetry in coiling implies also an asymmetry in mantle growth. Therefore, we can put our modeling framework to the test by studying the ornamentation morphology of shells with asymmetric coiling. In particular, we are motivated by a striking feature found in some brachiopod shells, as shown in Fig. 7. These shells exhibit a secondary, long wavelength pattern, on top of which a small wavelength primary pattern can be found[‡]. Both the long and short wavelength patterns vary significantly between species and specimens, yet remarkably, perfect interlocking is maintained in all cases.

To study the impact of asymmetry in the model we suppose that one valve, say valve 1, has a higher secretion rate than the other one, say valve 2. The corresponding mismatch in mantle growth means that mantle 1 will have a greater (unstressed) reference length, but is under the same geometric constraints as mantle 2. This mismatch induces a mechanical stress in the mantle tissue which is relieved by a secondary buckling instability of the entire mantle/periostacum tissue[§].

C.1. Adaptive accretion. As a first test of the model, we check that interlocking is maintained within the framework we have

[‡]We term the long wavelength pattern as secondary, as this pattern only ever appears later in development, while the small scale ornamentation appears early and has the same characteristics as the ornamentations we have described thus far in this paper.

[§]In this view, the small scale pattern is primarily focussed at the thin periostacum while the much thicker mantle remains effectively flat; see SI Appendix Section 5 and SI Appendix Fig. 2.

443 developed. In the base case, before any deformation, the
 444 coiling rates are constant for each valve, and the two valve
 445 edges meet at the same mid-plane when the valves are closed.
 446 Once a large-scale deformation occurs, the valve edges no
 447 longer meet in a single plane (the $x - y$ plane as in the base
 448 case). Some material points along the edge will have moved
 449 in one direction (to $z > 0$ say) while other points will have
 450 moved the other direction ($z < 0$). However, the rotation of
 451 each valve about the hinge – increased rotation is needed to
 452 accommodate increased material – is a *global* property. Thus,
 453 the geometrical constraint of the presence of the opposing valve
 454 *locally* changes along the shell edge. The local accretion rate,
 455 i.e. local coiling rate, must change in response. By analysing
 456 the coiling geometry with such a deformation imposed, we
 457 show in SI Appendix Section 5 that the coiling naturally adapts
 458 such that the two shell edges still perfectly coincide, though
 459 no longer in a single plane.

460 The next step is to reintroduce the small-scale pattern
 461 by the same process as before: a generative zone strain is
 462 induced by the difference in arclength at the valleys compared
 463 to the peaks of the small-scale pattern, and thus the plane
 464 of ornamentation is defined such that the arclength is equal
 465 at the peaks and valleys. The corresponding nonlinear ODE
 466 is then solved for the tilt of mantle that defines the local
 467 plane of ornamentation (details in SI Appendix Section 5A).
 468 The net result is that the plane of ornamentation rotates non-
 469 uniformly at each point along the shell edge compared to the
 470 base case, but the orientations still coincide locally between
 471 the two valves. Thus Rule 1 is satisfied even in the presence
 472 of asymmetry.

473 **C.2. Synchrony of ornamentation with asymmetry.** The conceptual
 474 idea of Rule 2 is as before: for interlocking to occur the
 475 ornamentation patterns must be antisymmetric, a synchrony
 476 we expect to be maintained by the mutual interaction of the
 477 mantles. However, the situation is more complicated by the
 478 difference in mantle growth rates and requires an extension of
 479 the previous mechanical model for two mantles geometrically
 480 constrained by each other with the additional assumption that
 481 they are growing at unequal rates (see SI Appendix Section
 482 6).

483 We find that for moderate asymmetry, the interaction of
 484 the mantles is sufficient to enforce synchrony of the pattern.
 485 However, as further elucidated in SI Appendix Section 6,
 486 for larger asymmetry the mantles eventually separate due
 487 to a divergence in their reference lengths. A bio-mechanical
 488 coupling would be necessary in such cases.

489 **C.3. Asymmetry patterns.** We confirm the prediction of our
 490 model against basic morphological trends observed in shells
 491 with the secondary pattern. In Brachiopods the two valves
 492 cover the dorsal and ventral sides of the animal. Prior to the
 493 large-scale deformation, the dorsal side has the higher coiling
 494 rate (when there is asymmetry present). Once the large scale
 495 pattern appears, the following characteristics are observed:

- 496 (i) The large wavelength pattern appears either as an “even
 497 mode” or an “odd mode” (see Fig. 7(c)).
- 498 (ii) There is a positive correlation between the degree of
 499 dorso-ventral asymmetry and the size of the large-scale
 500 pattern.

501 Observation (i) is clearly compatible with a mechanical
 502 instability, for which different buckling modes will be triggered
 503 based on geometric and mechanical parameters. For odd
 504 modes, there is no lateral preference, i.e. right and left “handed”
 505 shells with an odd mode always occur in roughly the same
 506 numbers in populations (?) and in the 29 known cases
 507 of plant and animal displaying random direction of bilateral
 508 asymmetry, the direction of asymmetry almost always lacks
 509 a genetic basis (?). A mechanical origin is consistent with
 510 this trend, as there is no lateral preference in the case of
 511 an odd mode buckling, by symmetry of the geometry. With
 512 even modes, on the other hand, the middle point of the shell
 513 edge *always* deforms towards the dorsal valve. This requires a
 514 bias in the buckling direction that only impacts even modes;
 515 a plausible mechanism based on the already present coiling
 asymmetry is described in SI Appendix Section 6.

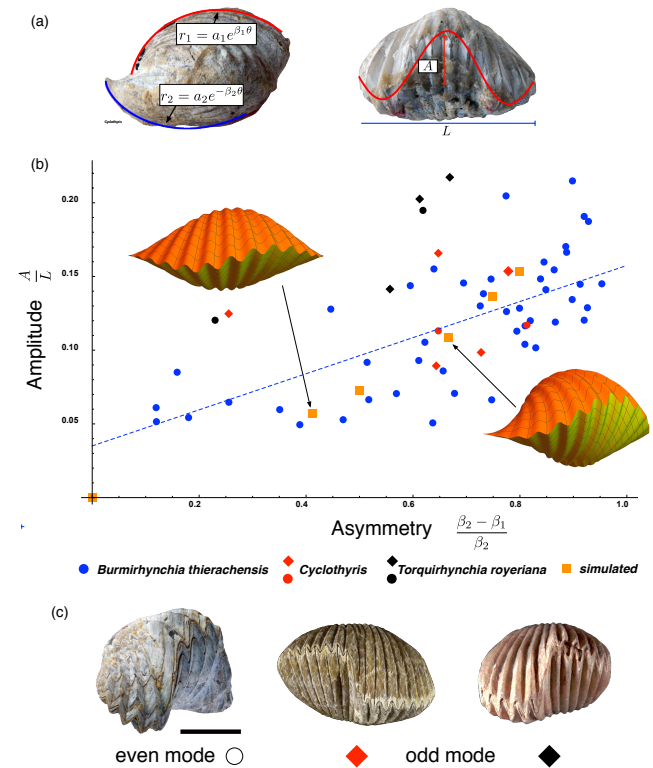


Fig. 7. Asymmetry and large-scale pattern in brachiopods. (a) For each shell we extract both *asymmetry* measure via difference in coiling rates and relative *amplitude* of the large pattern. (b) These data are collected on a set of shells displaying the large scale pattern: *Burmirthynchia thierachensis* (blue), *Cyclothyris* (red), and *Torquirhynchia royeriana* (black). Shells displaying odd mode are marked with a diamond symbol. A linear regression is plotted as the dashed line. The orange squares are produced via a two-beam mechanical model, and complete shells are simulated at the marked points. (The hollow point at the origin is not simulated; by construction zero asymmetry has zero amplitude.) (c) Large wavelength patterns in Brachiopods appear both as an “even mode” deformation (left: *Septaliphoria orbignyana*) and “odd mode” (middle: *Cyclothyris* sp. and right: *Torquirhynchia royeriana*). In the latter, there is no lateral preference.

516 Observation (ii) is also consistent with a mechanical process,
 517 as an increase in dorso-ventral asymmetry would imply an
 518 increase in mechanical stress, which would lead to earlier
 519 buckling and an increased amplitude relative to shell size. To
 520 quantify this trend, we have studied a sample of 59 brachiopods
 521 from different species. For each shell, we extract dorso-ventral
 522

523 asymmetry by fitting a logarithmic spiral to a side profile, 524 and amplitude of the large pattern by fitting a sinusoid to 525 a front view, as shown in Fig. 7(a). Amplitude is plotted 526 against asymmetry in Fig. 7(b), showing a strong correlation: 527 we compute a Spearman's rank correlation coefficient of 0.67, 528 and a p-Value less than 0.0001. The extracted data, as well 529 as an image of every shell sampled with curves overlaid, is 530 available in SI Appendix Section 7. From the mechanical model 531 (SI Appendix Section 6) we extract the equivalent measures 532 by taking the difference in asymmetry to correspond to the 533 difference in mantle growth rates, computing the bifurcation 534 curves following buckling and extracting amplitude relative 535 to length for several different measures of asymmetry. These 536 appear as the orange squares in Fig. 7(b), demonstrating that 537 the patterns and trends predicted by the model are consistent 538 with the observed morphological trends.

539 Moreover, the morphological features are well captured 540 by the model. To illustrate, the computed buckled shape at 541 the two marked simulated points in Fig. 7(b) was fed into 542 the full shell model, with small pattern taken as output of 543 the small-scale mechanical model and plane of ornamentation 544 computed with adapted coiling in combination with base shell 545 geometry; all model components combined to produce the 546 simulated shells appearing in Fig. 7(b), which in both cases 547 exhibit a perfect interlocking.

548 4. Discussion

549 In this paper we have shown the key role of mechanics in form- 550 ing common features of shell sculpture in interlocking bivalved 551 shells. Ornamentation appears as a mechanical instability 552 arising due to a simple developmental change – growth of the 553 mantle outpacing expansion of the aperture – while at the 554 same time shell interlocking is maintained by mechanical forces 555 without requiring specific genetic processes. This biophysical 556 explanation of developmental origins provides a much-needed 557 complementary view to functional considerations. Indeed, during 558 the 20th century most aspects of brachiopods and mollusk 559 shells morphologies have been interpreted within the functional 560 perspective of the neo-Darwinian synthesis. According to this 561 view one may explain how a trait has come into being and 562 has evolved by appealing to its function alone. For instance, 563 Rudwick (28) proposed that zigzag-shaped commissures have 564 evolved as filtering grids to prevent the entry of harmful parti- 565 cles above a certain size in brachiopods and bivalves that feed 566 by filtering tiny food particles from seawater, and concluded 567 that this function explains the presence of this trait and the 568 intrinsic probability that zigzags evolved many times independ- 569 ently in these organisms, an interpretation that has since 570 remained unquestioned (29, 30). However, the promotion of 571 traits by natural selection is logically distinct from the mecha- 572 nisms that generate them during development. While some of 573 the possible functional advantages of interlocking structures 574 are clear, an explanation of the repeated emergence of similar 575 characters in distantly related lineages requires an understand- 576 ing of the development of these characters that might induce 577 a reproductive bias (i.e. natural selection).

578 Our study shows that a part of the morphological diver- 579 sity and evolution of these groups of invertebrates may be 580 understood in light of both the mechanical interactions of the 581 mantle with the rigid shell edge, and the reciprocal mechanical 582 influence that both mantle lobes have on each other during

583 shell secretion. Our conclusion is that brachiopods and bi- 584 valves have managed to secrete interlocking shells simply as a 585 consequence of a biaxially constrained mechanical instability 586 of the secreting mantle. It is therefore not surprising that the 587 same patterns of interlocking structures have evolved repeat- 588 edly among brachiopods and bivalves, an evolutionary trend 589 which is a predictable outcome of the physics of the growth 590 process. It is also worth noting that we have restricted our 591 study to self-similar shell growth (prior to emergence of any 592 large-scale pattern) and with small-scale patterns appearing 593 at right angles to the shell margin. While it is a suitable as- 594 sumption for most bivalves and brachiopods, there are species 595 that deviate from self-similarity or with ribs appearing oblique 596 to the shell margin. In such shells interlocking is consistently 597 maintained, suggesting that the process we propose is robust 598 with respect to these perturbations as well. Accordingly, we 599 hypothesize that mechanical forces also play the same role in 600 these systems. However, to model these forces explicitly 601 would require introducing an additional torsional component 602 in the generative zone[¶] and/or deviating from the self-similar 603 growth that we have utilized in our geometric construction. 604 While such steps are certainly feasible, and conceptually all of 605 the same ideas outlined in our paper would still apply, mod- 606 elling such cases would introduce additional computational 607 complexity and is left as future work.

608 There are other striking examples in nature of organisms 609 with matching of body parts, such as the closed mouth of 610 the snapdragon flower (? ?), the interacting gears of the 611 planthopper insect *Issus* (?), or dental occlusion in vertebrates 612 (?). The role of mechanics in the morphogenesis of such 613 structures could be the subject of fruitful future inquiries. 614 Among mollusks, the hinge in bivalves is also formed by a 615 series of interlocking teeth and sockets on the dorsal, inner 616 surface of the shell. In this case too, the hinge teeth are 617 secreted by two lobes of the mantle which are retracted from 618 the hinge line when the shell is tightly closed and when teeth 619 and sockets interlock in each other. The morphology of these 620 hinge teeth (e.g. taxodont, heterodont, schizodont...) have 621 traditionally provided the basis of bivalve classifications, but 622 recent molecular phylogenies (?) show that these characters 623 do not always bear a coherent phylogenetic signal, which could 624 be explained by the fact that ahistorical physical processes 625 play an important role in their development.

626 The fact that physical processes are key in shell morphogen- 627 esis does not imply that genetic and molecular processes are 628 irrelevant. For example, both the amplitude and wavelength 629 of ornamentation may vary considerably among oyster species, 630 possibly because of species-specific combinatorial variations 631 in control parameters such as commarginal growth rate or 632 stiffness of the mantle. Given that these parameters may be 633 genetically modulated, our approach might open the door to 634 future studies aiming at understanding how biochemical and 635 biophysical processes across scales could conspire to regulate 636 the development and variations of morphologies among dif- 637 ferent species. The interplay between predictable patterns 638 and unpredictability of specific outcomes in large part defines 639 biological evolution (?). Cells, tissues, and organs satisfy 640 the same laws of physics as non-living matter, and in focusing 641 on the noncontingent and predictable rules that physical pro-

[¶]In terms of the plane of ornamentation, our model considers a rotation about the tangent d_3 direction; an oblique pattern could be produced by also rotating about the d_2 direction, which would create a 'slant' to the antimarginal ornamentation

642 cesses introduce in development and in the trajectories that
643 are open to morphological evolution, we shift the focus from
644 the Darwinian perspective of “the survival of the fittest”, to a
645 more predictive one of “the making of the likeliest”.

646 While buckling and wrinkling instabilities have long been
647 viewed as only detrimental in engineering, an increasing num-
648 ber of studies, often inspired by biology, have shown the
649 potential contribution of this physical phenomenon to smart
650 applications (?). Interlocking structures are ubiquitous in
651 man-made structures where they serve as physical connections
652 between constitutive parts in such diverse areas as building
653 or biomedical engineering, and their presence in nature is a
654 source of inspiration for biomimetic engineering (?). Our
655 study shows that brachiopods and bivalves have made good
656 use of mechanical instabilities to secrete their interlocking shell
657 since about 540 million years; in this light perhaps the growth
658 of these invertebrates could be inspirational in biomimetic re-
659 search for the development of self-made interlocking structures
660 at many scales.

661 **Data availability**

662 All materials, methods, and data needed to evaluate the con-
663 clusions are present in the main article and/or SI Appendix.